Transactions of the 14th International Conference on Structural Mechanics in Reactor Technology (SMiRT 14), Lyon, France, August 17-22, 1997 F04/4

Last improvements on the ratchetting interaction diagram method

Riou B.[1], Ponter A.R.S.[2], Carter K.F.[2], Guinovart J.[3]
(1) Framatome, France
(2) University of Leicester, United Kingdom
(3) Commission of the European Communities, Belgium

ABSTRACT

This paper describes the last improvements brought on the ratchetting interaction diagram method and presents a procedure for use by designers together with its background. An example of application based on a typical LMFR structure subject to a sodium moving free level is carried out. A complement to design code rules is the use of the mechanisms approach to ratchet limits and the four distinct deformation types, which have been identified as covering almost the entire solution set of ratchet limits, are presented.

1 - INTRODUCTION

The structures of Liquid Metal Fast Reactors (LMFRs) are subjected to cyclic loads consisting of low primary stresses and significant thermal stresses. Their design is to be checked against ratchetting but design rules available are not always well appropriate in particular for cases with zero primary load (e.g. sodium moving free level problem).

The ratchetting interaction diagram method has been developed by LEICESTER University. This method provides a graphical representation of the ratchetting boundary as a function of the primary and secondary stresses. The method was originally developed in terms of secondary stress intensity but a recent work, carried out by LEICESTER University and FRAMATOME in the frame of the activities of the Working Group on Codes and Standards of DG XI/C (Nuclear Safety of Installations), proposed a modification of the method in order to enable secondary stress ranges to be used [1].

This paper describes the improvements brought on the ratchetting interaction diagram method and presents a procedure for use by designers. The background to this procedure is provided and an example of application based on a typical LMFR structure subject to a sodium moving free level is carried out. It also presents the mechanisms approach to ratchet limits which should represent a complement to design code rules.

2 - INTERACTION DIAGRAM METHOD

The aim of the interaction diagrams is to provide a graphical representation of ratchet

boundary as a function of the thermal stress and the primary stress. This boundary is obtained using the upper bound shakedown theorem for the shakedown/ratchet boundary and the extended upper bound shakedown theorem for the ratchet boundary into the reverse plasticity region [2].

A computer code called TUBCON was developed at Leicester University for studying the structural behaviour of cylindrical shells subjected to cyclic thermal loads and mechanical loads. This computer code was used for providing a set of interaction diagrams for a large range of temperature distributions including through wall temperature gradients as well as moving or stationary axial gradients. Figures 1 shows examples of interaction diagrams. For case (a), the through thickness temperature gradient is completely dominant, thus the ratchetting boundary is close to the Bree Line. For case (b), the axial temperature gradient is dominant resulting in ratchetting at zero mechanical load. Case (c) shows the effects of movement of a predominantly axial temperature gradient over a significant length, causing ratchetting at low levels of the thermal load.

Parametric studies involving the analysis of several thousand cases indicated that by the introduction of a modest amount of conservatism, these diagrams could be condensed to produce just two ratchetting interaction diagrams, one for situations where the cyclic thermal gradient is solely through wall (Bree case) and the other for situations involving axial cyclic thermal gradients as well. These two diagrams form the basis for the interaction diagram method.

3 - GENERAL DESCRIPTION OF THE INTERACTION DIAGRAM PROCEDURE

3.1 - *Limitation on use*

The procedure is applicable for an axisymmetric and near cylindrical thin shell and assumes that the primary stresses are suitably limited to avoid P-type damage.

The rules have been set up on the basis of thermal stresses. They may however be extended to any secondary stresses under the condition that the membrane axial stress (which is zero for thermal loads) is conservatively taken into account by classifying the maximum value as primary.

3.2 - *Input data to the method*

The input data are the maximum values within the shell of the following quantities :

* the membrane plus bending primary stress, max ($\overline{P_L + P_b}$) (or max ($\overline{P_m + P_b}$)),
* the secondary stress range, max($\overline{\Delta Q}$),
* the membrane secondary stress range, max($\overline{\Delta Q_m}$),
* the temperature, max θ.

As ratchetting may be a global and not only a local phenomenon, these quantities should not be necessarily correlated in space.

3.3 - *Severity factor F*

As noted in section 2, for situations involving axial temperature gradient, there may be ratchetting at zero mechanical load. For simplicity reasons it has been decided to define for such cases the ratchetting boundary in the interaction diagram as a straight line passing through the points (1,0) and (0,F) where F is the allowable non-dimensional secondary stress at zero mechanical load.

In the previous version of the rule written in terms of stress intensity, F had been obtained by defining the relationship between F and G = maximum thermal stress / maximum membrane thermal stress for which the line passing through the points (1,0) and (0,F) corresponded to the lowest envelope of any situation that may occur. F was defined on the basis of several thousand interaction diagrams. The resulting value of F was however rather conservative in the sense that it covered situations with moving temperature front with rather long movements ("long travel" cases) for which the allowable secondary stress at zero mechanical load was very low. It is unlikely that such cases would occur on real structures.

The F factor was defined as follows :

$F = 0.9\ G$	$G \le A$	(A=2.5)
$F = 0.9\ \sqrt{A\ G}$	$G > A$	and $\gamma = 1$
$F = 0.9\ \sqrt[3]{A^2 G}$	$G > A$	and $\gamma > 1$

where γ is a scaling factor on the ratchetting boundary (in the ordinate direction):

. $\gamma = 1$ if the through wall temperature gradient does not undergo cyclic reversal,

. $\gamma = 2$ if the through wall temperature gradient undergoes complete cyclic reversal,

and with G increased by a factor of 2 for stationary temperature distributions.

In the process of defining the new F value with rules written in terms of secondary stress ranges, the same formulation was kept for F and the parameter A was adjusted so as to give the most appropriate response. The resulting formulation is :

for $G = \max(\overline{\Delta Q}) / \max(\overline{\Delta Q_m})$	$F=1.8\ G$	$G \le A$	(A=1.5)
	$F=1.8\sqrt[3]{A^2 G}$	$G > A$	

It has been shown that with this formulation the F factor was conservative compared to the interaction diagrams except in a few extreme cases where a very shallow temperature gradient over a long length of tube is allowed to cyclically move over a relatively short length of cylinder. This unconservatism would be obtained for high values of the non-dimensional secondary stress corresponding in fact to unrealistic values of θ max (greater than 800°C).

Moreover, this new formulation together with the all procedure has been tested on VINIL experiments carried out at CEA Cadarache and gave results fully satisfactory compared with experimental results.

3.4 - *Effects of changing the yield stress with temperature*

Temperature dependent yield stress can have a very important role in determining the boundaries with an interaction diagram. This is taken into account conservatively by considering the yield stress corresponding to the maximum temperature within the shell throughout the operational cycle.

3.5 - *Effects of strain hardening*

Interaction diagrams have been built up assuming an elastic perfectly plastic behaviour law. The effect of strain hardening is taken into account by replacing the yield stress by $K_1 (R_{0.002})_{min}$, where $K_1 (R_{0.002})_{min}$ is the effective yield strength of the material defined as the largest stress which satisfies two criteria, namely strain growth ceases within 500 cycles of application and total strain accumulation less than 2 per cent.

3.6 - *Non-dimensional parameters*

The procedure uses non-dimensional parameters defined as follows :

* non-dimensional primary stress $$C = \frac{\max(\overline{P_L + P_b})}{K_1 (R_{0.002})_{min}}$$

* non-dimensional secondary stress range $$\Delta T = \frac{\max(\overline{\Delta Q})}{K_1 (R_{0.002})_{min}}$$

3.7 - *Interaction diagrams and structural behaviour assessment*

As stated in section 2, two diagrams are used in the interaction diagram method.

The first one (figure 2) corresponds to the Bree case which involves only through wall temperature gradients. The diagram corresponds therefore to cases where the secondary loading is purely bending.

The second one (figure 3) enables to take into account loadings with membrane secondary loading including problems of temperature front moving axially along the shell.

The structural behaviour is acceptable (free from ratchetting) if the loading point (C, ΔT) lies within the allowable domain.

3.8 - *Procedure for checking the effects of creep*

The method consists in assuming that any point on the ratchetting boundary must give a value of creep reference stress σ_r equal to the yield stress of the material σ_y for the corresponding value of the reference temperature.

Consequently the actual creep reference stress for a particular loading point $\underline{L}$ (C,ΔT) will be a linear scaling of that point from the origin $\underline{0}$ (0,0) to the ratchetting boundary $\underline{L}^*$ (C*,ΔT*), where the points $\underline{0}$, $\underline{L}$ and $\underline{L}^*$ lie on a straight line, giving :

$$\sigma_r = \sigma_y |\underline{L}| / |\underline{L}^*|,$$

with σ_y equal to $K_1 (R_{0.002})_{min}$ in order to take into account the strain hardening effect.

The mechanism of creep deformation will be the same as that of the corresponding point $\underline{L}^*$ on the ratchetting boundary. This observation is then used to find a value for the creep reference temperature. This is done by integrating the maximum value of the temperature at any point within the structure $\theta_{max}(\underline{X})$ during the thermal loading cycle, over the region in

which the plastic deformation strain εP occurs. In practice it is found that the value of the reference temperature calculated using the above approach is almost always the maximum temperature found anywhere within the structure. The main exception to this is where the thermal loading is Bree like (i.e. thermal bending stresses only) when the reference temperature takes the mean value of the through-wall temperature. The justification for this procedure and comparisons with available creep data are discussed at length in [3].

The values of the creep reference stress and reference temperature are then used together with the appropriate isochronous creep curves for the material to obtain the accumulated creep strain in a given time or the time for the structure to amass a given amount of creep strain.

Values of allowable accumulated strain of 2 % for parent metal and 1 % for weld metal are used.

4 - EXAMPLE OF APPLICATION OF THE INTERACTION DIAGRAM PROCEDURE

The example of application consists in a thin shell (internal radius of 8000 mm and thickness of 20 mm) in the area of a moving Na free level.

This shell is subjected to a thermal load consisting in a load change from 30 % to 100 % of the nominal power. No mechanical load is present. The load change is associated with an upward movement of the Na free level by 110 mm. This problem involves an important axial temperature gradient in the shell. The through thickness gradient is negligible.

The maximum secondary stress range max ($\overline{\Delta Q}$) and membrane secondary stress ranges max ($\overline{\Delta Q_m}$) are obtained between the beginning and the end of the transient and reaches respectively 252 and 222 MPa. The associated temperature profiles are shown in figure 4.

The application of the interaction diagram procedure leads to the following :

$C = 0$
$\Delta T = 1.65$ (with $K_1 = 1.35$ and $(R_{0.002})_{min} = 113.2$ MPa at 545 °C)
$G = 1.14$ which leads to $F = 2.04$

As $\Delta T < F$, the structural behaviour is acceptable. The procedure for checking the effects of creep leads to an accumulated strain of 0.31 % over a total hold time of 280,000 h at 545 °C which is acceptable for parent metal as well as for weld metal.

5 - THE MECHANISMS APPROACH

A complement to design code rules is the use of the mechanisms approach to ratchet limits. It has been shown that, despite the considerable range of thermal histories and the different elastic stresses associated with them, the range of mechanisms which characterises the ratchet boundaries is quite narrow. Four distinct deformation types have been identified as covering almost the entire solution set of ratchet limits. For each of the mechanisms types, the upper bound shakedown theorem is used to derive algebraic expressions of the corresponding solution. Interaction diagrams may then be formed from sections which correspond to the

mechanisms which yields the lowest mechanical load for the prescribe temperature history. A full description of the derivation of the mechanisms equations is found in [1].

5.1 - *Mechanisms 1 and 2*

Mechanisms 1 and 2 are, essentially, local mechanisms consisting of a plane strain axial extension over a short length of the cylinder and, as a result, refer to extreme stresses occurring at any point along the cylinder's length. Mechanism 1 is the Bree Mechanism, expressed in terms of the maximum axial bending stress. Mechanism 2 is a reverse plasticity mechanism where the variation of hoop stress produces plastic strains at the extremes of the thermal stress history, producing a net zero hoop strain but a non-zero axial strain. Both these mechanism equations depend upon the thermoelastic stress range.

5.2 - *Mechanisms 3 and 4*

Mechanisms 3 and 4 consist of global mechanisms where a length of tube deforms either outwards (Mechanism 3) or inwards (Mechanism 4) with two linear regions of membrane stretching connected by axial plastic hinges. In the case of Mechanism 3 the deformation is entirely radial whereas in Mechanism 4 there is a combination of both radial and axial deformation. In both cases the thermal stresses over a length of cylinder are involved and it becomes necessary to introduce simplifying and bounding assumptions concerning the thermoelastic stress history to allow the derivation of algebraic expressions. The result is given for the case were the maximum axial bending stress is assumed to act, with an appropriate sign, at each of the plastic hinges (see figure 5). The length of cylinder involved is defined by assuming a bounding value of the maximum positive hoop stress extending over a length Δs. The primary load is applied as an axial load. The following argument does not, in fact, depend upon these precise details, but they simplify the discussion.

With these assumptions the relationship between the primary stress σ_p , the maximum membrane stress $\overline{\sigma_m}$ and the maximum bending stress $\overline{\sigma_b}$ is given for Mechanism 3 by :

$$\frac{\sigma_x{}^p}{\sigma_y} = 1 - (\overline{\sigma_\phi} / \sigma_y) / \left(1 + \left(\frac{4}{\overline{\Delta s}^2} \right) \frac{(1 - 2\overline{\sigma_x}^b / 3\sigma_y)^2}{(\overline{\sigma_\phi} / \sigma_y)} \right) \qquad (1)$$

where $\overline{\sigma_\phi} = \overline{\sigma_\phi}^m + \overline{\Delta\sigma_\phi}^b / 4$ and $\overline{\Delta s} = \Delta s / \sqrt{Rt}$

There are two features of this equation which are of particular interest. The variation of σ_p with $\overline{\Delta s}$ indicates that for small values of $\overline{\Delta s}$ then $\sigma_p = \sigma_y$, i.e. the effect of thermoelastic stresses are insignificant in determining the load factor for Mechanism 3 under these conditions, i.e. other mechanisms may have a lower load factor associated with them.

For $\overline{\Delta s}$ significantly greater than 2 we reach the "long travel " limit of :

$$\frac{\sigma_x{}^p}{\sigma_y} = 1 - \left(\frac{\overline{\sigma_\phi}^m}{\sigma_y} + \frac{\overline{\Delta\sigma_\phi}^b}{4\sigma_y} \right) \qquad (2)$$

This equation has the simple interpretation that the membrane component of the hoop stresses

acts as a primary stress. A corresponding argument for mechanism 4 produces similar result.

Assuming $\overline{\sigma_\phi}^m >> \overline{\Delta\sigma_\phi}^b$ and $\overline{\sigma_\phi}^m = \max(\overline{\Delta Q_m})/2$, equation (2) may be written with the notations of the interaction diagram procedure as :

$$C = 1 - \Delta T / 2G \qquad (3)$$

which means that the allowable thermal stress range corresponding to zero mechanical load F = 2 G, which is conservative compared to the interaction diagram procedure.

Assuming in addition that $\overline{\sigma_x}^b \approx \overline{\sigma_\phi}^m$ gives that equation (1) may be written as :

$$C = 1 - \frac{\Delta T}{2G} \Big/ \left(1 + \frac{4}{\overline{\Delta s}^2}\left(\frac{2G}{\Delta T} - \frac{2}{3}\right)\right) \qquad (4)$$

Figure 6 compares equations (3) and (4) for cases corresponding to G = 1.2 and enables to quantify for one specific case the benefit that could be brought from the use of the mechanisms approach. Note that realistic values for $\overline{\Delta s}$ are around 2.

6 - CONCLUSIONS

The last improvement brought on the ratchetting interaction diagram method have been described and a procedure for use by designers has been proposed.

This procedure is applicable for dealing with industrial problems and an example of application based on a typical LMFR structure has been presented.

A complement to design code rules is the use of the mechanisms approach. This approach can be used as a theoretical support to the interaction diagram method and could be used for providing a less conservative estimate for ratchetting boundaries.

ACKNOWLEDGEMENTS

The authors wish to thank colleagues from AEA Technology who have contributed to this work.

REFERENCES

1. Ponter, A.R.S, K.F. Carter & B. Riou. Design rules for cylindrical shells subjected to axisymmetric temperature histories. Final report to contract RA1-0224-UK.
2. Ponter, A.R.S, S. Karadeniz & K.F. Carter. The computation of shakedown limits for structural components subjected to variable thermal loading - Brussels diagrams. Final report Contract RAP-054-UK. University of Leicester (Report EUR 12686 EN)
3. Ponter, A.R.S, A.C.F. Cocks. Computation of shakedown limits for structural components (Brussels diagrams) Part II - The creep range. Final report Contract RAP-066-UK (AD).

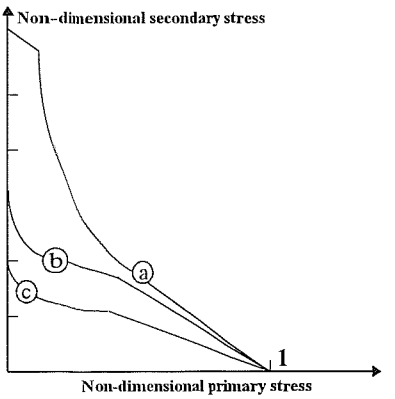

Figure 1 : Examples of interaction diagrams

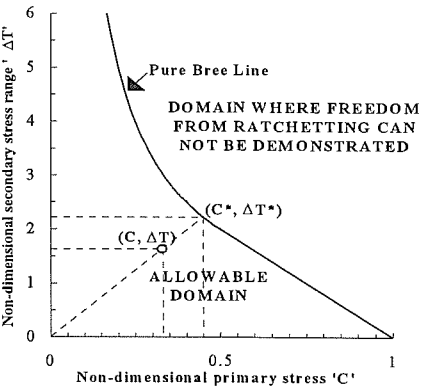

Figure 2 : Ratchetting interaction diagram (pure bending)

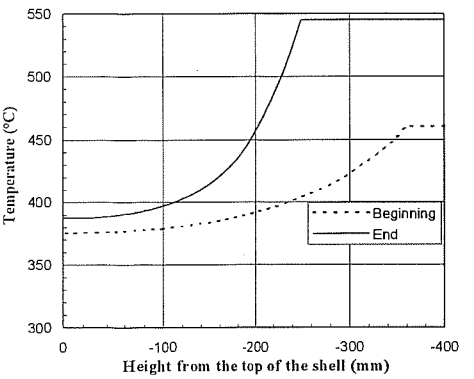

Figure 4 : Temperature profile during the load change

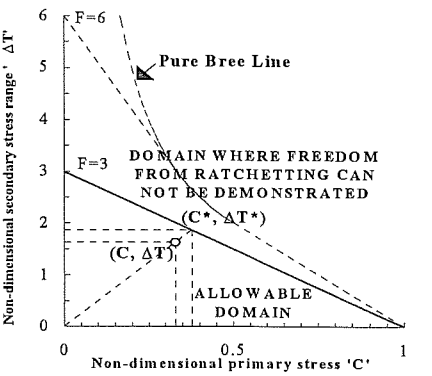

Figure 3 : Ratchetting interaction diagram (membrane + bending)

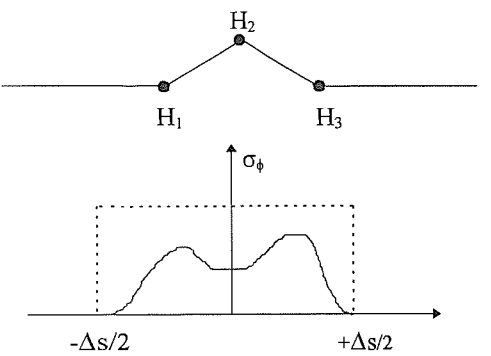

Figure 5 : Mechanism 3

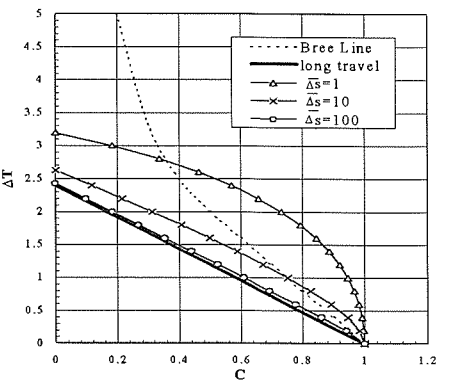

Figure 6 : Comparison between mechanism 3 and the « long travel » case